Journal of Pharmaceutical and Biomedical Analysis 55 (2011) 996–1009

Contents lists available at ScienceDirect

Journal of Pharmaceutical and Biomedical Analysis

journal homepage: www.elsevier.com/locate/jpba

Rapid profiling and identification of triterpenoid saponins in crude extracts from *Albizia julibrissin* Durazz. by ultra high-performance liquid chromatography coupled with electrospray ionization quadrupole time-of-flight tandem mass spectrometry

Lifeng Han[a], Guixiang Pan[a], Yuefei Wang[a], Xinbo Song[a], Xiumei Gao[a,*], Baiping Ma[b], Liping Kang[a,b]

[a] *Tianjin State Key Laboratory of Modern Chinese Medicine, Tianjin University of Traditional Chinese Medicine, No. 88 Yuquan Road, Tianjin 300193, PR China*
[b] *Beijing Institute of Radiation Medicine, No. 27 Taiping Road, Beijing 100850, PR China*

ARTICLE INFO

Article history:
Received 9 December 2010
Received in revised form 31 March 2011
Accepted 2 April 2011
Available online 8 April 2011

Keywords:
Albizia julibrissin Durazz.
UHPLC/ESI-Q-TOF
Triterpenoid saponins
Identification

ABSTRACT

Ultra high-performance liquid chromatography coupled with electrospray ionization quadrupole time-of-flight tandem mass spectrometry (UHPLC/ESI-Q-TOF-MS/MS) was applied to separate and identify triterpenoid saponins in crude extract from the stem bark of *Albizia julibrissin* Durazz. The molecular weights were determined by comparing quasi-molecular ions $[M+NH_4]^+$ in positive mode and $[M-H]^-$ and $[M-2H]^{2-}$ ions in negative mode. The MS/MS spectra of the $[M-H]^-$ ions for saponins provided a wealth of structural information related to aglycone skeletons, sugar types and linked sequence. On the basis of the fragmentation behavior of known saponins isolated before, saponins from this plant were identified, even though references were not available. As a result, a total of twenty-eight saponins in the crude extract were identified, which all had a common basic skeleton of the triterpene oleanolic acid and eight of them were new compounds.

1. Introduction

The stem bark of *Albizia julibrissin* Durazz. (Leguminosae) (Albizziae cortex), which is distributed across China, Africa, Mid Asia, East Asia and North America, is used as a sedative and anti-inflammatory agent, for treating injuries due to fall and removing carbuncles. It is widely used for treating insomnia together with other Traditional Chinese Medicine, such as Polygoni multiflori caulis and Ganoderma [1]. In modern pharmacology, it exhibits antitumor, immunomodulatory and anti-platelet activating factor receptor activities [2].

In previous studies, some saponins [3–21], lignanoids [22–24], flavonoids [2,25] and other compounds [24,26] were investigated and the major compounds were saponins. More than sixty triterpenoid compounds have been isolated from this genus, some of which were reported to have significant cytotoxic and antitumor activites [2–21]. Most aglycones are of the oleanolic acid type, which are substituted with oligosaccharides at C-3, C-21 and C-28 to form trisdesmosidic triterpene saponins and the saccharide sequences are highly homologous. On the sugar chain at C-28, all saponins are substituted with Glc–(1 → 3)–[Ara–(1 → 4)]–Rha–(1 → 2)–Glc. The sugar chain at C-3 on the other hand has six possibilities, Xyl–Ara/Fuc–Glc, Xyl–Ara/Fuc–Glc(2-NHAC) and Xyl–Ara/Fuc–(Glc)–Glc. For the sugar chain at C-21, there are only two types of sugars (either Qui or Xyl). Although several saponins were identified [2–21], the isolation works was tedious due to their high polarity. Moreover, the structure elucidation of saponins is also difficult, especially when the sugar chain contains more than three residues.

Several analytical methods have been reported on saponins using LC–MS, including ion trap and Q-TOF mass spectrometry [27,28]. UHPLC offers significant advantages in resolution, speed, reproducibility and sensitivity for analysis with little solvent consumption [29]. In addition, the combination of UHPLC and Q-TOF technique could give excellent separating and good structural characterization abilities which make it suitable to analyze complex extracts in Traditional Chinese Medicine [28].

The aim of this study was to develop a UHPLC/ESI-Q-TOF-MS/MS method for effectively profiling and identifying triterpenoid saponins (Fig. 1).

* Corresponding author at: Tianjin University of Traditional Chinese Medicine, Tianjin 300193, PR China.
E-mail addresses: hanlifeng_1@sohu.com (L. Han), gaoxiumei@tjutcm.edu.cn (X. Gao).

0731-7085/$ – see front matter © 2011 Elsevier B.V. All rights reserved.
doi:10.1016/j.jpba.2011.04.002

2. Materials and methods

2.1. Reagents and chemicals

HPLC grade acetonitrile (Merck KGaA, Darmstadt, Germany) and analytical grade ammonium formate (Sinopharm Chemical Reagent Co., Ltd, China) were utilized for the UHPLC analysis. Deionized water was purified using a Milli-Q system (Millipore, Bedford, MA, USA). All other chemicals were of analytical grade.

Eight standard compounds, prosapogenin-9, prosapogenin-12, julibroside J_{25}, julibroside J_{20}, prosapogenin-3, prosapogenin-4, prosapogenin-10 and julibroside J_{22}, were isolated and purified from the stem bark of *A. julibrissin* by the authors. Their structures were determined by the analysis of UV, IR, 1D, 2D NMR, MS spectra and compared with previous literature [3,7]. The structural elucidation and isolation procedure for prosapogenin-9, 12, 3 and 10 was reported in a recent article [30]. The purities of isolates were over 95%, determined by HPLC/ELSD analysis based on a peak area

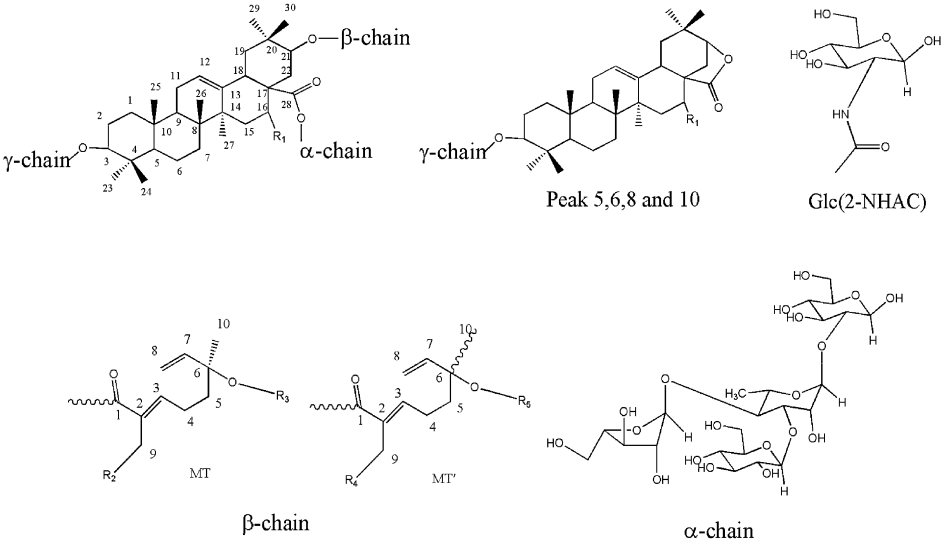

Compounds	R_1	γ–chain	β–chain	MW
julibroside J_{20}	OH	Xyl(1→2)Ara(1→6)Glc	Xyl(1→6)MT(C_9-OH)	1830.8299
julibroside J_{22}	OH	Xyl(1→2)Ara(1→6)Glc(2-NHAC)	Xyl(1→6)MT(C_9-OH)	1885.8721
julibroside J_{25}	OH	Xyl(1→2)Ara(1→6)Glc	Qui(1→6)MT(C_9-OH)	1844.8455
prosapogenin-10	OH	Xyl(1→2)Fuc(1→6)Glc	Qui(1→6)MT(C_9-OH)	1858.8612
prosapogenin-4	OH	Xyl(1→2)Ara(1→6)Glc(2-NHAC)	–	937.5035
prosapogenin-3	OH	Xyl(1→2)Ara(1→6)Glc	–	896.4770
Isomer of J_{26}*	OH	Xyl(1→2)Ara(1→6)Glc	Xyl(1→6)MT	1828.8506
julibroside J_{A3}	OH	Xyl(1→2)Fuc(1→6)Glc(2-NHAC)	–	951.5192
New compound*	H	Xyl(1→2)Ara(1→6)Glc	Qui(1→6)MT	1812.8557
julibroside J_{A2}	OH	Xyl(1→2)Fuc(1→6)Glc	–	910.4926
prosapogenin-12	H	Xyl(1→2)Fuc(1→6)[Glc(1→2)]Glc	Qui(1→6)MT	1988.9242
prosapogenin-9	OH	Xyl(1→2)Fuc(1→6)Glc	Qui(1→6)MT	1842.8663
prosapogenin-11	H	Xyl(1→2)Fuc(1→6)Glc	Qui(1→6)MT	1826.8714
Isomer of J_5*	OH	Xyl(1→2)Fuc(1→6)Glc	Qui-(6R)MT'-Qui-MT(C_9-OH)	2171.0185
Isomer of J_8*	OH	Xyl(1→2)Fuc(1→6)Glc	Qui-(6R)MT'-Qui-MT(C_9-OH)	2171.0185

Fig. 1. Chemical structures of the identified triterpenoid saponins from Albizziae coxtex (* compounds are new).

julibroside J_1	OH	Xyl(1→2)Ara(1→6)Glc	Qui(1→6)(6R)MT'(1→4)Qui(1→6)MT(C_9-OH)	2157.0028
julibroside J_9	OH	Xyl(1→2)Ara(1→6)Glc	Qui(1→6)(6S)MT'(1→4)Qui(1→6)MT(C_9-OH)	2157.0028
julibroside J_{14}	OH	Xyl(1→2)Ara(1→6)Glc	Qui(1→6)(6R)MT'(1→4)Qui(1→6)MT	2141.0079
julibroside J_{15}	OH	Xyl(1→2)Ara(1→6)Glc	Qui(1→6)(6S)MT'(1→4)-Qui(1→6)MT	2141.0079
julibroside J_5	OH	Xyl(1→2)Fuc(1→6)Glc	Qui(1→6)(6R)MT'(1→4)Qui(1→6)MT(C_9-OH)	2171.0185
julibroside J_8	OH	Xyl(1→2)Fuc(1→6)Glc	Qui(1→6)(6S)MT'(1→4)Qui(1→6)MT(C_9-OH)	2171.0185
Isomer of J_{16}*	OH	Xyl(1→2)Fuc(1→6)Glc	Qui-(6R)MT'-Qui-MT	2155.0236
julibroside J_{35}	OH	Xyl(1→2)Ara(1→6)Glc	Xyl(1→6)(6R)MT'(1→4)Qui(1→6)MT	2126.9923
julibroside J_{16}	OH	Xyl(1→2)Fuc(1→6)Glc	Qui(1→6)(6R)MT'(1→4)-Qui(1→6)MT	2155.0236
Isomer of J_{14}*	OH	Xyl(1→2)Ara(1→6)Glc	Qui-(6R)MT'-Qui-MT	2141.0079
Isomer of J_{15}*	OH	Xyl(1→2)Ara(1→6)Glc	Qui-(6S)MT'-Qui-MT	2141.0079
Isomer of J_4*	OH	Xyl(1→2)Fuc(1→6)Glc	Qui(1→6)(6S)MT'(1→4)-Qui(1→6)MT	2155.0236
julibroside J_4	OH	Xyl(1→2)Fuc(1→6)Glc	Qui(1→6)(6S)MT'(1→4)-Qui(1→6)MT	2155.0236

Fig. 1. (*Continued*).

normalization method. The standard solution of each saponin was prepared by dissolving it in 50% (v/v) methanol and stored at 4 °C until analysis.

2.2. LC–MS

UHPLC analyses were performed on an Agilent 1290 UHPLC instrument (Agilent, Waldbronn, Germany) coupled to a binary pump, a diode-array detector, an autosampler, and a column thermostat. The sample was separated on an Agilent RRHD SB-C18 column (1.8 μm, 100 × 2.1 mm; Agilent Technologies, USA). The mobile phase consisted of CH_3CN (solvent A) and H_2O (containing 1 mM $HCOONH_4$; solvent B). A gradient program was used according to the following profile: 0–10 min, 25% A; 10–35 min, 25–33% A; 35–60 min, 33–38% A; 60–65 min, increased to 80% A; 65–70 min, decreased to 25% A. The flow rate was 0.4 ml min^{-1} and the column temperature set at 45 °C.

Aglient 6520 Q-TOF mass spectrometer (Agilent Corp., Santa Clara, CA, USA) was connected to the Agilent 1290 UHPLC instrument via an ESI interface. The acquisition parameters were as follows: drying gas (N_2) flow rate, 8.0 l/min; temperature, 360 °C; nebulizer, 30 psig; capillary, 4500 V; fragmentor, 300 V; skimmer, 65 V; OCT RF V, 750 V. Each sample was analyzed in both positive and negative ion mode to provide complimentary information for molecular formulae and structural identification.

The quasi-molecular ion $[M-H]^-$ of interest in the negative ESI mode MS scan was selected as precursor ion and subjected to Target-MS/MS analyses. The collision energy (CE) was set at 50–80 V and the mass range recorded *m*/*z* 100–3000.

2.3. Plant material and sample preparation

The stem bark of *A. julibrissin* was collected from the Sichuan Province, People's Republic of China, in August 2006. The plant was identified by Prof. Lijuan Zhang, and a voucher specimen (No. 061001) deposited in the Herbarium of the Beijing Institute of Radiation Medicine, Beijing. For the preparation of all extracts, 200 g of Albizziae cortex was extracted with 10 folds of 50% (v/v) ethanol by refluxing for 2 h. The extract was then subjected to chromatography over the macroporous resin AB-8 (100 g) and eluted with water (400 ml), 30% ethanol (400 ml), 50% ethanol (400 ml) and 80% ethanol (400 ml) sequentially to give four fractions. The 80% ethanol fraction was evaporated to dryness. An aliquot of obtained residue (1 mg) was dissolved in 1 ml 50% (v/v) methanol solution. After centrifugation at 13,200 × *g* for 10 min, the supernatant was transferred to an autosampler vial for UHPLC/ESI-Q-TOF-MS/MS analysis.

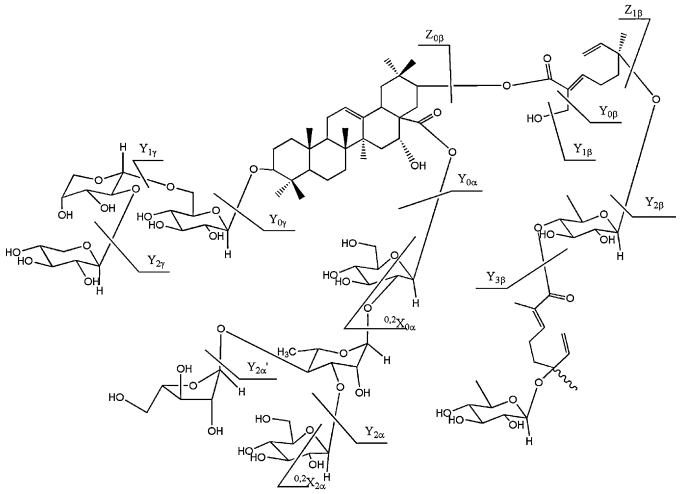

Fig. 2. The fragmentation nomenclature of julibroside J_1.

Table 1
ESI-TOF-MS data of compounds identified from the extract from *A. julibrissin*.

Peak	RT (min)	Formula	Selected ion	*m/z* experimental	*m/z* calculated	Error (ppm)
1	4.08	$C_{84}H_{134}O_{43}$	$[M-H]^-$	1829.822	1829.8226	0.3
			$[M-2H]^{2-}$	914.4058	914.4077	0.84
			$[M+NH^4]^+$	1848.8606	1848.8637	1.31
2	5.63	$C_{87}H_{139}NO_{43}$	$[M-H]^-$	1884.8628	1884.8648	0.83
			$[M-2H]^{2-}$	941.9276	941.9288	0.59
			$[M+NH^4]^+$	1903.9043	1903.9059	0.89
			$[M+H]^+$	1886.8792	1886.8794	0.66
			$[M+Na]^+$	1908.8661	1908.8613	−1.35
3	6.60	$C_{85}H_{136}O_{43}$	$[M-H]^-$	1843.836	1843.8383	0.92
			$[M-2H]^{2-}$	921.4136	921.4155	1.15
			$[M+NH^4]^+$	1862.8801	1862.8794	−0.03
4	13.54	$C_{86}H_{138}O_{43}$	$[M-H]^-$	1857.8523	1857.8539	0.6
			$[M-2H]^{2-}$	928.4219	928.4233	0.52
			$[M+NH^4]^+$	1876.8949	1876.895	0.36
5	15.51	$C_{48}H_{75}NO_{17}$	$[M-H]^-$	936.4961	936.4962	0.07
			$[M+H]^+$	938.5098	938.5108	1.25
			$[M+Na]^+$	960.4916	960.4927	1.16
6	17.68	$C_{46}H_{72}O_{17}$	$[M-H]^-$	895.4697	895.4697	−0.03
			$[M+Cl]^-$	931.4466	931.4464	0.25
			$[M+HCOO]^-$	941.4748	941.4752	0.41
			$[2M-H]^-$	1791.9433	1791.9466	3.01
			$[M+NH^4]^+$	914.511	914.5108	−0.24
7	19.67	$C_{85}H_{136}O_{42}$	$[M-H]^-$	1827.8425	1837.8433	0.45
			$[M-2H]^{2-}$	913.4167	913.418	0.7
			$[M+NH^4]^+$	1846.8832	1846.8844	0.81
8	21.54	$C_{49}H_{77}NO_{17}$	$[M-H]^-$	950.512	950.5119	−0.18
			$[M+Cl]^-$	986.4867	986.4886	2.47
			$[M+HCOO]^-$	996.5175	996.5174	−0.17
			$[M+H]^+$	952.5261	952.5264	0.38
			$[M+Na]^+$	974.5082	974.5084	0.2
9	23.10	$C_{85}H_{136}O_{41}$	$[M-H]^-$	1811.8465	1811.8484	0.84
			$[M-2H]^{2-}$	905.419	905.4206	0.9
			$[M+NH^4]^+$	1830.8884	1830.8895	0.62
10	24.07	$C_{47}H_{74}O_{17}$	$[M-H]^-$	909.4853	909.4853	0.1
			$[M+Cl]^-$	945.4613	945.462	0.86
			$[M+HCOO]^-$	955.491	955.4908	−0.16
			$[2M-H]^-$	1819.9754	1919.9719	2.6
			$[M+NH^4]^+$	928.5261	928.5264	−0.22
11	24.77	$C_{92}H_{148}O_{46}$	$[M-H]^-$	1987.9128	1987.9169	2.06
			$[M-2H]^{2-}$	993.4536	993.4548	0.7
			$[M+NH^4]^+$	2006.9549	2006.958	1.11
12	24.98	$C_{86}H_{138}O_{42}$	$[M-H]^-$	1841.8623	1841.859	−1.7
			$[M-2H]^{2-}$	920.426	920.4259	−0.02
			$[M+NH^4]^+$	1860.8979	1860.9001	1.19
13	27.49	$C_{86}H_{138}O_{41}$	$[M-H]^-$	1825.8627	1825.8641	0.57
			$[M-2H]^{2-}$	912.4277	912.4284	0.26
			$[M+NH^4]^+$	1844.9039	1844.9052	0.77
14	28.32	$C_{102}H_{162}O_{49}$	$[M-H]^-$	2170.0062	2170.0112	2.28
			$[M-2H]^{2-}$	1084.499	1084.502	1.3
			$[M+NH^4]^+$	2189.0534	2189.0523	−0.06
15	28.69	$C_{102}H_{162}O_{49}$	$[M-H]^-$	2170.008	2170.0112	0.96
			$[M-2H]^{2-}$	1084.5002	1084.502	0.66
			$[M+NH^4]^+$	2189.051	2189.0523	0.5
16	31.89	$C_{101}H_{160}O_{49}$	$[M-H]^-$	2155.9931	2155.9955	0.74
			$[M-2H]^{2-}$	1077.4926	1077.4941	0.64
			$[M+NH^4]^+$	2175.0387	2175.0366	−0.87
17	32.67	$C_{101}H_{160}O_{49}$	$[M-H]^-$	2155.9936	2155.9955	0.93
			$[M-2H]^{2-}$	1077.4923	1077.4941	0.67
			$[M+NH^4]^+$	2175.037	2175.0366	0.18
18	34.35	$C_{101}H_{160}O_{48}$	$[M-H]^-$	2139.9991	2140.0006	0.7
			$[M-2H]^{2-}$	1069.4947	1069.4967	0.96
			$[M+NH^4]^+$	2159.0409	2159.0417	0.23
19	34.70	$C_{101}H_{160}O_{48}$	$[M-H]^-$	2139.9995	2140.0006	0.99
			$[M-2H]^{2-}$	1069.4958	1069.4967	0.32
			$[M+NH^4]^+$	2159.0413	2159.0417	0.16
20	36.10	$C_{102}H_{162}O_{49}$	$[M-H]^-$	2170.0118	2170.0112	0.68
			$[M-2H]^{2-}$	1084.5019	1084.502	−0.02
			$[M+NH^4]^+$	2189.058	2189.0523	−2.42
21	36.89	$C_{102}H_{162}O_{49}$	$[M-H]^-$	2170.0076	2170.0012	−1.66
			$[M-2H]^{2-}$	1084.5002	1084.499	−0.51
			$[M+NH^4]^+$	2189.0531	2189.0523	−0.31
22	38.91	$C_{102}H_{162}O_{48}$	$[M-H]^-$	2154.0093	2154.0163	4.41
			$[M-2H]^{2-}$	1076.5018	1076.5045	1.19
			$[M+NH^4]^+$	2173.056	2173.0574	0.77

Table 1 (*Continued*).

Peak	RT (min)	Formula	Selected ion	*m/z* experimental	*m/z* calculated	Error (ppm)
23	39.26	$C_{100}H_{158}O_{48}$	$[M-H]^-$	2125.9856	2125.985	0.57
			$[M-2H]^{2-}$	1062.4879	1062.4889	0.34
			$[M+NH^4]^+$	2145.0289	2145.0261	−1.26
24	39.29	$C_{102}H_{162}O_{48}$	$[M-H]^-$	2154.0128	2154.0163	1.34
			$[M-2H]^{2-}$	1076.5025	1076.5045	0.96
			$[M+NH^4]^+$	2173.058	2173.0574	−0.02
25	41.58	$C_{101}H_{160}O_{48}$	$[M-H]^-$	2140.0007	2140.0006	0.34
			$[M-2H]^{2-}$	1069.4959	1069.4967	0.46
			$[M+NH^4]^+$	2159.0505	2159.0417	−3.58
26	42.52	$C_{101}H_{160}O_{48}$	$[M-H]^-$	2139.9969	2140.0006	1.74
			$[M-2H]^{2-}$	1069.4954	1069.4967	1.19
			$[M+NH^4]^+$	2159.0449	2159.0417	−1.05
27	46.89	$C_{102}H_{162}O_{48}$	$[M-H]^-$	2154.0114	2154.0163	1.15
			$[M-2H]^{2-}$	1076.5035	1076.5045	0.59
			$[M+NH^4]^+$	2173.0583	2173.0574	−0.55
28	47.93	$C_{102}H_{162}O_{48}$	$[M-H]^-$	2154.0123	2154.0163	1.94
			$[M-2H]^{2-}$	1076.5023	1076.5045	0.98
			$[M+NH^4]^+$	2173.0581	2173.0574	−0.24

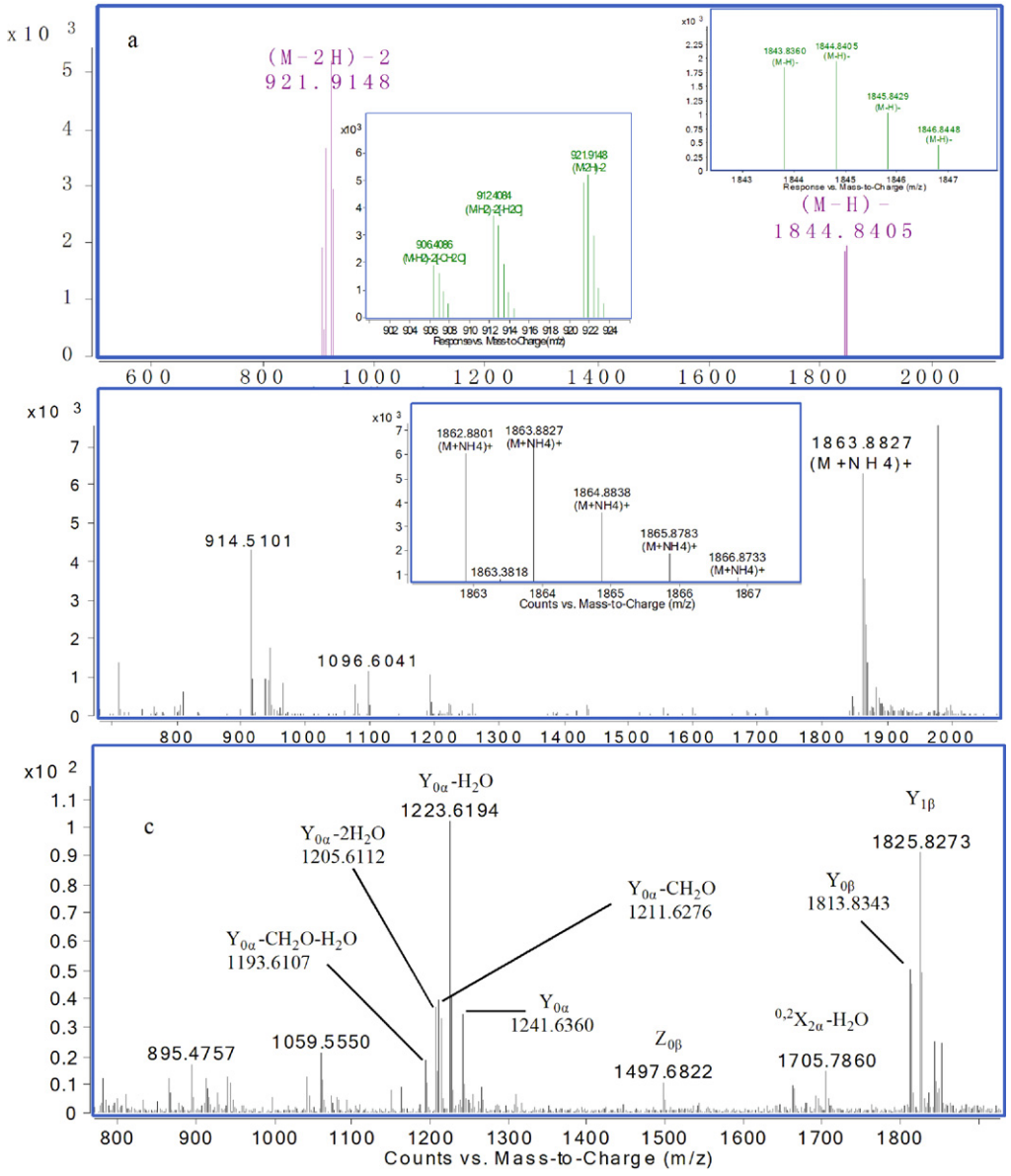

Fig. 3. ESI-MS spectra of peak 3: (a) (−) ESI-MS; (b) (+) ESI-MS; (c) MS/MS of the $[M-H]^-$ ion.

Table 2
MS/MS data of compounds identified from the extract from *A. julibrissin*.

Peak	(−) ESI-MS m/z	MS/MS (m/z)	Structural elucidation
1	1829.8226 $[M-H]^-$	1811.8205 ($Y_{1\beta}$), 1799.8046 ($Y_{0\beta}$), 1209.6102 ($Y_{0\alpha}-H_2O$), 1227.6130 ($Y_{0\alpha}$), 1191.6025 ($Y_{0\alpha}-2H_2O$), 1197.5998 ($Y_{0\alpha}-CH_2O$), 1661.7591 ($Z_{1\beta}-H_2O$), 1179.5981 ($Y_{0\alpha}-CH_2O-H_2O$)	Julibroside J_{20}
2	1884.8648 $[M-H]^-$	1866.8645 ($Y_{1\beta}$), 1854.8424 ($Y_{0\beta}$), 1264.6402 ($Y_{0\alpha}-H_2O$), 1252.6587 ($Y_{0\alpha}-CH_2O$)	Julibroside J_{22}
3	1843.8383 $[M-H]^-$	1825.8273 ($Y_{1\beta}$), 1813.8343 ($Y_{0\beta}$), 1223.6194 ($Y_{0\alpha}-H_2O$), 1241.6360 ($Y_{0\alpha}$), 1205.6112 ($Y_{0\alpha}-2H_2O$), 1211.6276 ($Y_{0\alpha}-CH_2O$), 1661.7604 ($Z_{1\beta}-H_2O$), 1497.6822 ($Z_{0\beta}$), 1193.6107 ($Y_{0\alpha}-CH_2O-H_2O$), 1705.7860 ($^{0,2}X_{2\alpha}-H_2O$)	Julibroside J_{25}
4	1857.8539 $[M-H]^-$	1839.8435 ($Y_{1\beta}$), 1827.8449 ($Y_{0\beta}$), 1237.6359 ($Y_{0\alpha}-H_2O$), 1255.6470 ($Y_{0\alpha}$), 1225.6372 ($Y_{0\alpha}-CH_2O$), 1219.6257 ($Y_{0\alpha}-2H_2O$), 1675.7640 ($Z_{1\beta}-H_2O$), 1511.6988 ($Z_{0\beta}$), 1207.6244 ($Y_{0\alpha}-CH_2O-H_2O$), 1719.8091 ($^{0,2}X_{2\alpha}-H_2O$)	Prosapogenin-10
5	936.4961 $[M-H]^-$	804.4513 ($Y_{2\gamma}$)	Prosapogenin-4
6	895.4697 $[M-H]^-$	763.4311 ($Y_{2\gamma}$), 631.3849 ($Y_{1\gamma}$)	Prosapogenin-3
7	1827.8433 $[M-H]^-$	1707.8170 ($^{0,2}X_{2\alpha}$), 1225.6395 ($Y_{0\alpha}$), 1207.6256 ($Y_{0\alpha}-H_2O$)	3-*O*-[β-D-xylopyranosyl-(1 → 2)-α-L-arabinopyranosyl-(1 → 6)-β-D-glucopyranosyl]-21-*O*-[(6*S*)-2-*trans*-2,6-dimethyl-6-*O*-(β-D-quinovopyranosyl)-2,7-octadienoyl]-acacic acid -28-*O*-β-D-glucopyranosyl-(1 → 3)-[α-L-arabinofuranosyl-(1 → 4)]-α-L-rhamnopyranosyl-(1 → 2)-β-D-glucopyranosyl ester
8	950.5119 $[M-H]^-$	818.4668 ($Y_{2\gamma}$), 672.4178 ($Y_{1\gamma}$)	Julibroside J_{A2}
9	1811.8484 $[M-H]^-$	1691.8123 ($^{0,2}X_{2\alpha}$), 1679.8031 ($Y_{2\alpha'}$), 1649.8068 ($Y_{2\alpha}$), 1209.6418 ($Y_{0\alpha}$)	3-*O*-[β-D-xylopyranosyl-(1 → 2)-α-L-arabinopyranosyl-(1 → 6)-β-D-glucopyranosyl]-21-*O*-[(6*S*)-2-*trans*-2,6-dimethyl-6-*O*-(β-D-quinovopyranosyl)-2,7-octadienoyl]-16-deoxy-acacic acid -28-*O*-β-D-glucopyranosyl-(1 → 3)-[α-L-arabinofuranosyl-(1 → 4)]-α-L-rhamnopyranosyl-(1 → 2)-β-D-glucopyranosyl ester
10	909.4853 $[M-H]^-$	777.4449 ($Y_{2\gamma}$), 631.3895 ($Y_{1\gamma}$)	Julibroside J_{A3}
11	1987.9169 $[M-H]^-$	1385.6923 ($Y_{0\alpha}$), 1841.8601 ($Y_{2\beta}$), 1239.6732 ($Y_{0\alpha}$–Qui)	Prosapogenin-12
12	1841.8590 $[M-H]^-$	1239.6516 ($Y_{0\alpha}$), 1221.6393 ($Y_{0\alpha}-H_2O$), 1721.8153 ($^{0,2}X_{2\alpha}$),1679.8168 ($Y_{2\alpha}$)	Prosapogenin-9
13	1825.8641 $[M-H]^-$	1705.8217 ($^{0,2}X_{2\alpha}$), 1693.8029 ($Y_{2\alpha'}$), 1663.8107 ($Y_{2\alpha}$), 1223.6561 ($Y_{0\alpha}$)	Prosapogenin-11
14	2170.0112 $[M-H]^-$	2151.9997 ($Y_{1\beta}$), 2139.9917 ($Y_{0\beta}$), 1839.8460 ($Y_{3\beta}$), 1821.8443 ($Y_{3\beta}-H_2O$), 1549.7921 ($Y_{0\alpha}-H_2O$), 1537.7968 ($Y_{0\alpha}-CH_2O$), 1531.7877 ($Y_{0\alpha}-2H_2O$), 1519.8107 ($Y_{0\alpha}-CH_2O-H_2O$), 1567.7959 ($Y_{0\alpha}$), 1237.6316 ($Y_{3\beta}-H_2O-\alpha$-chain), 1219.6330 ($Y_{3\beta}-2H_2O-\alpha$-chain)	Isomer of J_5
15	2170.0112 $[M-H]^-$	2152.0000 ($Y_{1\beta}$), 2140.0077 ($Y_{0\beta}$), 1839.8395 ($Y_{3\beta}$), 1821.8381 ($Y_{3\beta}-H_2O$), 1549.7950 ($Y_{0\alpha}-H_2O$), 1537.8011 ($Y_{0\alpha}-CH_2O$), 1531.7869 ($Y_{0\alpha}-2H_2O$), 1519.7949 ($Y_{0\alpha}-CH_2O-H_2O$), 1567.8103 ($Y_{0\alpha}$), 1237.6379 ($Y_{3\beta}-H_2O-\alpha$-chain), 1219.6237 ($Y_{3\beta}-2H_2O-\alpha$-chain)	Isomer of J_8
16	2155.9955 $[M-H]^-$	2137.9871 ($Y_{1\beta}$), 2125.9958 ($Y_{0\beta}$), 1807.8125 ($Y_{3\beta}-H_2O$), 1825.8276 ($Y_{3\beta}$), 1535.7845 ($Y_{0\alpha}-H_2O$), 1553.7896 ($Y_{0\alpha}$), 1523.7742 ($Y_{0\alpha}-CH_2O$), 1223.6271 ($Y_{3\beta}-H_2O-\alpha$-chain), 1205.6092 ($Y_{3\beta}-2H_2O-\alpha$-chain)	Julibroside J_1
17	2155.9955 $[M-H]^-$	2137.9645 ($Y_{1\beta}$), 2125.9839 ($Y_{0\beta}$), 1807.8353 ($Y_{3\beta}-H_2O$), 1825.8386 ($Y_{3\beta}$), 1535.7863 ($Y_{0\alpha}-H_2O$), 1553.7773 ($Y_{0\alpha}$), 1523.7514 ($Y_{0\alpha}-CH_2O$), 1223.6362 ($Y_{3\beta}-H_2O-\alpha$-chain), 1205.6188 ($Y_{3\beta}-2H_2O-\alpha$-chain)	Julibroside J_9
18	2140.0006 $[M-H]^-$	1809.8276 ($Y_{3\beta}-H_2O$), 1827.8531 ($Y_{3\beta}$), 1537.7960 ($Y_{0\alpha}$), 1519.7974 ($Y_{0\alpha}-H_2O$), 1225.6444 ($Y_{3\beta}-\alpha$-chain), 1207.6284 ($Y_{3\beta}-H_2O-\alpha$-chain)	Julibroside J_{14}
19	2140.0006 $[M-H]^-$	2121.9896 ($Y_{1\beta}$), 2109.9979 ($Y_{0\beta}$), 1809.8365 ($Y_{3\beta}-H_2O$), 1827.8395 ($Y_{3\beta}$), 1791.8334 ($Y_{3\beta}-2H_2O$), 1537.7986 ($Y_{0\alpha}$), 1519.7834 ($Y_{0\alpha}-H_2O$), 1225.6418 ($Y_{3\beta}-\alpha$-chain), 1207.6261 ($Y_{3\beta}-H_2O-\alpha$-chain)	Julibroside J_{15}
20	2170.0112 $[M-H]^-$	2152.0031 ($Y_{1\beta}$), 2139.9999 ($Y_{0\beta}$), 1821.8391 ($Y_{3\beta}-2H_2O$), 1839.8434 ($Y_{3\beta}-H_2O$), 1809.8250 ($Y_{3\beta}-CH_2O-H_2O$), 1549.7918 ($Y_{0\alpha}-H_2O$), 1567.8065 ($Y_{0\alpha}$), 1537.7995 ($Y_{0\alpha}-CH_2O$), 1237.6433 ($Y_{3\beta}-H_2O-\alpha$-chain)	Julibroside J_5
21	2170.0112 $[M-H]^-$	2152.0011 ($Y_{1\beta}$), 2139.9977 ($Y_{0\beta}$), 1821.8388 ($Y_{3\beta}-2H_2O$), 1839.8447 ($Y_{3\beta}-H_2O$), 1809.8215 ($Y_{3\beta}-CH_2O-H_2O$), 1549.7935 ($Y_{0\alpha}-H_2O$), 1567.8041 ($Y_{0\alpha}$), 1537.7942 ($Y_{0\alpha}-CH_2O$), 1237.6381 ($Y_{3\beta}-H_2O-\alpha$-chain)	Julibroside J_8
22	2154.0163 $[M-H]^-$	2135.9879 ($Y_{1\beta}$), 2124.0112 ($Y_{0\beta}$), 1823.8434 ($Y_{3\beta}-H_2O$), 1841.8620 ($Y_{3\beta}$), 1551.8030 ($Y_{0\alpha}$), 1533.7910 ($Y_{0\alpha}-H_2O$), 1239.6531 ($Y_{3\beta}-\alpha$-chain), 1221.6618 ($Y_{3\beta}-H_2O-\alpha$-chain)	Isomer of J_{16}

Table 2 (*Continued*).

Peak	(−) ESI-MS *m/z*	MS/MS (*m/z*)	Structural elucidation
23	2125.9850 $[M-H]^-$	1827.8550 ($Y_{3\beta}$), 1523.7807 ($Y_{0\alpha}$), 1225.6634 ($Y_{3\beta}$–α-chain), 1207.6324 ($Y_{3\beta}$–H_2O–α-chain)	Julibroside J_{35}
24	2154.0163 $[M-H]^-$	1823.8499 ($Y_{3\beta}$–H_2O), 1841.8663 ($Y_{3\beta}$), 1551.8087 ($Y_{0\alpha}$), 1533.7913 ($Y_{0\alpha}$–H_2O), 1239.6471 ($Y_{3\beta}$–α-chain), 1221.6496 ($Y_{3\beta}$–H_2O–α-chain).	Julibroside J_{16}
25	2140.0006 $[M-H]^-$	1809.8429 ($Y_{3\beta}$–H_2O), 1827.8547 ($Y_{3\beta}$), 1519.7858 ($Y_{0\alpha}$–H_2O), 1537.7996 ($Y_{0\alpha}$), 1225.6413 ($Y_{3\beta}$–α-chain), 1207.6300 ($Y_{3\beta}$–H_2O–α-chain)	Isomer of J_{14}
26	2140.0006 $[M-H]^-$	1809.8346 ($Y_{3\beta}$–H_2O), 1827.8587 ($Y_{3\beta}$), 1519.7891 ($Y_{0\alpha}$–H_2O), 1537.7935 ($Y_{0\alpha}$), 1225.6396 ($Y_{3\beta}$–α-chain), 1207.6267 ($Y_{3\beta}$–H_2O–α-chain)	Isomer of J_{15}
27	2154.0163 $[M-H]^-$	2124.0014 ($Y_{0\beta}$), 1823.8415 ($Y_{3\beta}$–H_2O), 1841.8666 ($Y_{3\beta}$), 1551.8095 ($Y_{0\alpha}$), 1533.8001 ($Y_{0\alpha}$–H_2O), 1239.6494 ($Y_{3\beta}$–α-chain), 1221.6378 ($Y_{3\beta}$–H_2O–α-chain)	Isomer of J_4
28	2154.0163 $[M-H]^-$	1823.8457 ($Y_{3\beta}$–H_2O), 1841.8621 ($Y_{3\beta}$), 1551.8111 ($Y_{0\alpha}$), 1533.8067 ($Y_{0\alpha}$–H_2O), 1239.6514 ($Y_{3\beta}$–α-chain), 1221.6416 ($Y_{3\beta}$–H_2O–α-chain)	Julibroside J_4

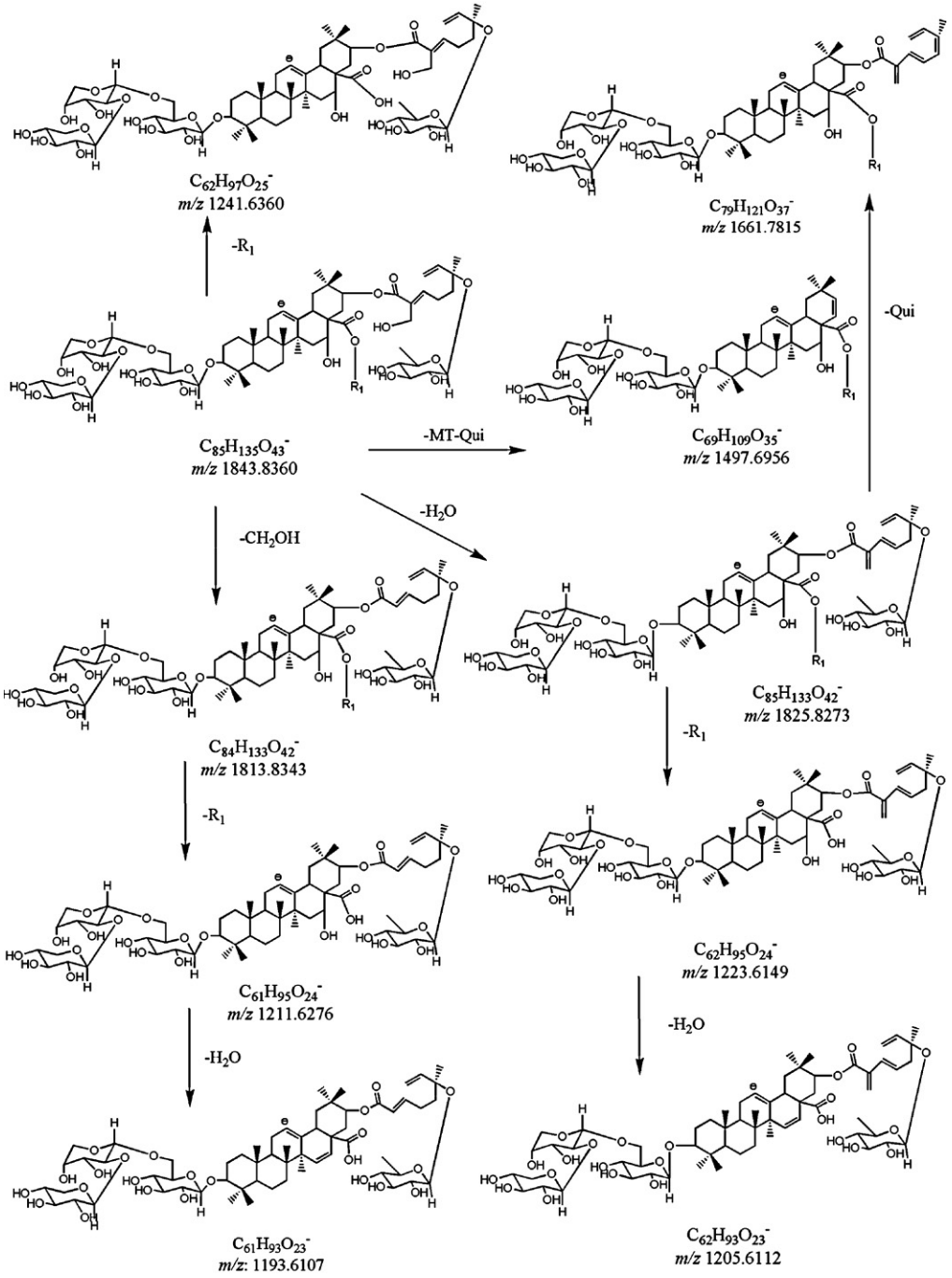

Fig. 4. Fragmentation pattern of peak 3.

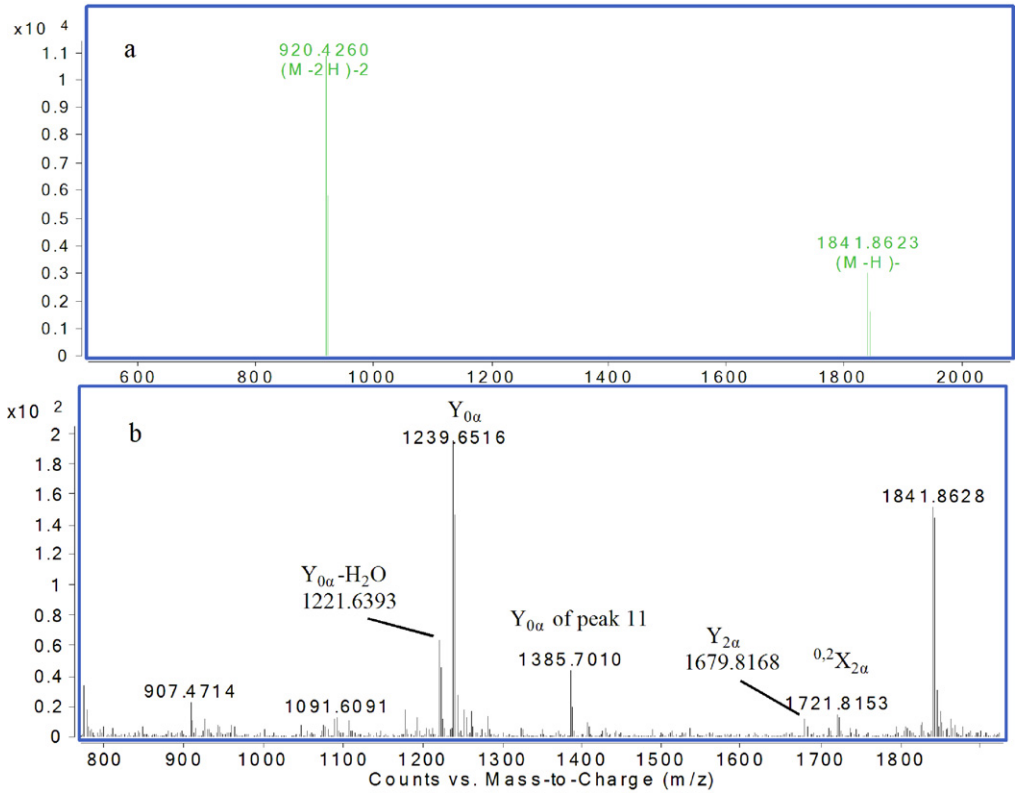

Fig. 5. ESI-MS spectra of peak 12: (a) ESI-MS; (b) MS/MS of the $[M-H]^-$ ion.

3. Results and discussion

3.1. LC-electrolyte effects and nomenclature

In the mobile phase, channel B contains 1 mM $HCOONH_4$, suitable ionisation of the saponins could be achieved in both positive and negative ESI-MS modes, probably due to the LC-electrolyte effects [31].

The Q-TOF-MS spectra were detected in both positive and negative ion modes. In the positive ion mode, the major ion specie generated was $[M+NH_4]^+$ and in the negative ion mode, the major ion species generated were $[M-H]^-$ and $[M-2H]^{2-}$. Although slightly greater sensitivity was achieved in the positive ion mode relative to the negative ion mode, the $[M+NH_4]^+$ ion produced a complex array of low abundance ions which were difficult to interpret. Therefore, the $[M-H]^-$ ion was selected for MS/MS analysis.

The nomenclature (julibroside J_1 as an example, Fig. 2) commonly used for triterpeniod saponins was adopted to denote the fragment ions to assist structural elucidation [27,32]. The ions retaining the charge on the main core structures were termed as Y and Z (glycosidic cleavages) and X (cross-ring cleavages). The Y ions were produced via the loss of sugar fragments and the Z ions, via the elimination of sugar moieties (see Fig. 2). Cross-ring cleavage ions were designated by superscript numbers indicating the two bonds cleaved. The oligosaccharide chain at C-28 was defined as the α-chain because the bond cleavage first occurred at this position under most MS/MS conditions, whereas the one at C-21 was defined as the β-chain and C-3 was γ-chain.

3.2. Proposed fragmentation pathway for albizia saponins

Fig. 3a presents the full-scan mass spectrum of peak 3 in negative ion mode. ESI-Q-TOF-MS analysis of 3 yielded $[M-H]^-$ and $[M-2H]^{2-}$ ions at *m/z* 1843.8360 and 921.4136 respectively. The $[M-2H-H_2O]^{2-}$ and $[M-2H-CH_2O]^{2-}$ ions at *m/z* 912.4084 and 906.4086 were observed at the same time. The $[M+NH_4]^+$ ion was observed at 1862.8801 in positive ion mode (Fig. 3b). In the MS/MS spectrum of $[M-H]^-$ (Fig. 3c), fragment ions at *m/z* 1825.8273, 1813.8343, 1223.6194, 1241.6360, 1205.6112, 1211.6276, 1661.7604, 1497.6822 and 1193.6107 corresponded to $Y_{1\beta}$, $Y_{0\beta}$, $Y_{0\alpha}$–H_2O, $Y_{0\alpha}$, $Y_{0\alpha}$–$2H_2O$, $Y_{0\alpha}$–CH_2O, $Z_{1\beta}$–H_2O, $Z_{0\beta}$ and $Y_{0\alpha}$–CH_2O–H_2O. The mass difference between the ions at *m/z* 1705.7860 and 1825.8273 is 120 Da, due to the cross-ring cleavage of one Glc ($^{0,2}X_{2\alpha}$–H_2O) (Fig. 4). Similar diagnostic fragmentation pattern was observed in the MS and MS/MS spectra of peak 2 and 4 (see Tables 1 and 2).

As with peak 1, the difference between 1 and 3 lies in the MT linked saccharide in the β-chain. In the structure of 1, Xyl links to the MT residue. While in the latter, the saccharide was Qui. Due to these differences, the $Z_{1\beta}$–H_2O ions which came from loss 132 + 18 + 18 Da of 1 and 146 + 18 + 18 Da of 3 respectively, should be same in the MS/MS spectrum. This feature, too, can be used to determine the structure of β-chain. The $[M-H]^-$, $[M-2H-H_2O]^{2-}$, $[M-2H-CH_2O]^{2-}$, $[M-2H]^{2-}$ and $[M+NH_4]^+$ ions were yielded at *m/z* 1829.8220, 905.4005, 899.4011, 914.4058 and 1848.8606. The $Y_{1\beta}$, $Y_{0\beta}$, $Y_{0\alpha}$–H_2O, $Y_{0\alpha}$, $Y_{0\alpha}$–$2H_2O$, $Y_{0\alpha}$–CH_2O, $Z_{1\beta}$–H_2O and $Y_{0\alpha}$–CH_2O–H_2O ions can be observed as similar to 3 (14 Da lower than that of 3).

As shown in Fig. 5a, peak 12 produced $[M-H]^-$ and $[M-2H]^{2-}$ ions at *m/z* 1841.8623 and 920.4260 in (−) ESI-MS. Whereas on the (+) ESI-MS, $[M+NH_4]^+$ was obtained at *m/z* 1860.8979. However the $[M-2H-H_2O]^{2-}$ and $[M-2H-CH_2O]^{2-}$ ions were not observed, this difference resulted in the MT residue. In the MS/MS spectrum, only four fragments [$Y_{2\alpha}$ (*m/z* 1679.8168), $^{0,2}X_{2\alpha}$ (*m/z* 1721.8153), $Y_{0\alpha}$ (*m/z* 1239.6516) and $Y_{0\alpha}$–H_2O (*m/z* 1221.6393)] were obtained (Fig. 5b). These fragment ions gave us a hint that the $Y_{1\beta}$, $Y_{0\beta}$,

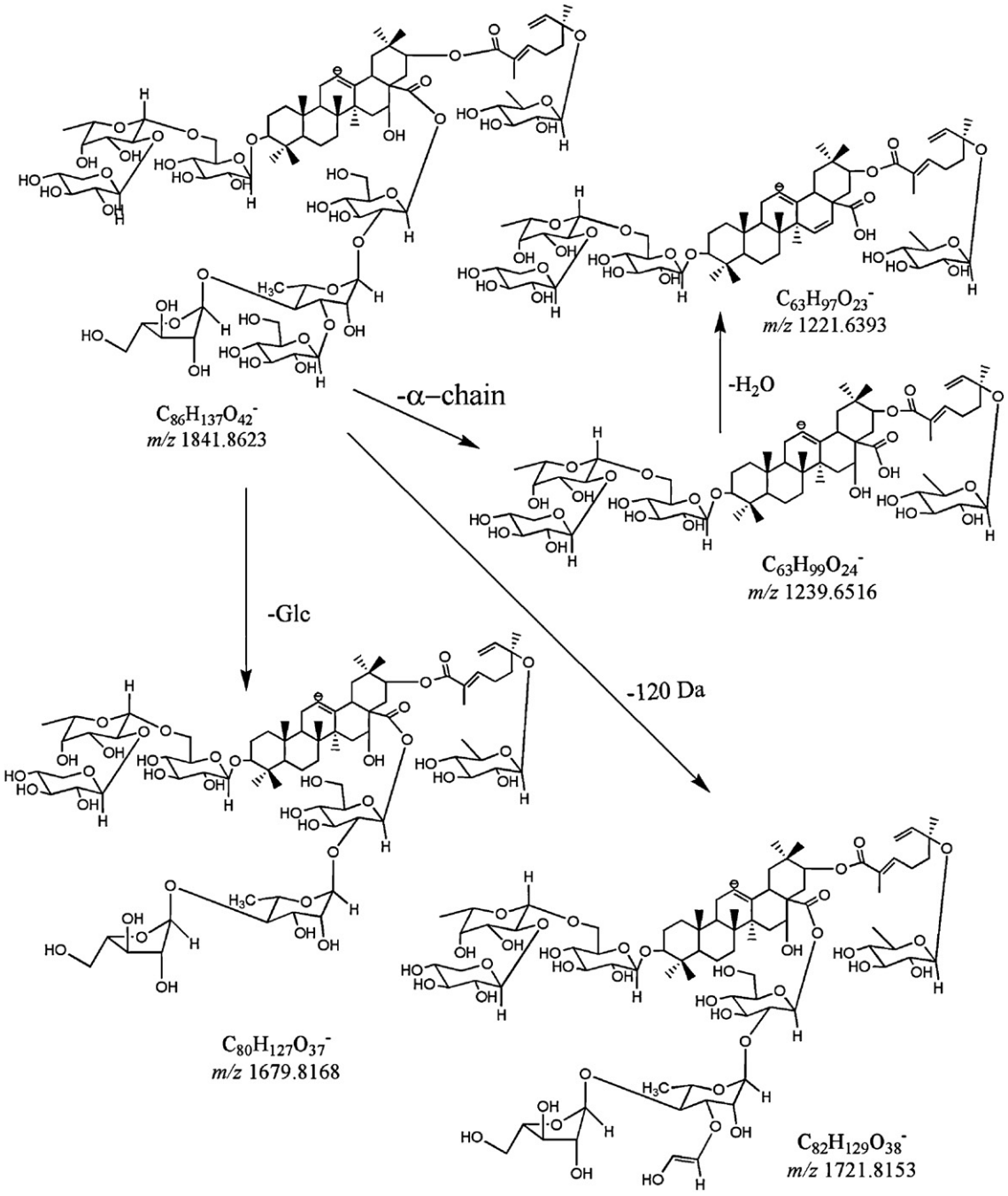

Fig. 6. Fragmentation pattern of peak 12.

$Z_{1\beta}$–H_2O and $Y_{0\alpha}$–CH_2O ions were related to MT residue (Fig. 6). Similar diagnostic fragmentation pattern was observed in the MS and MS/MS spectra of peak 11 (see Tables 1 and 2).

The $[M+H]^+$ (*m/z* 938.5098), $[M+Na]^+$ (*m/z* 960.4916) and $[M-H]^-$ (*m/z* 936.4961) for peak 5 and the $[M-H]^-$ (*m/z* 895.4697), $[M+Cl]^-$ (*m/z* 931.4466), $[M+HCOO]^-$ (*m/z* 941.4748) and $[M+NH_4]^+$ (*m/z* 914.5110) for peak 6 were observed. The fragmentation patterns of 6 and 5 are very simple, such as $Y_{2\gamma}$ (*m/z* 804.4513 and 763.4311) and $Y_{1\gamma}$ (*m/z* 631.3849).

From the above fragmentation rules can be deduced: when the MT residue possesses a C_9–OH, there must be a $[M-H-H_2O]^-$ ion as the base peak in the MS/MS of $[M-H]^-$, and when the MT residue does not possess the C_9–OH, the base peak is $[M-H-\alpha\text{-chain}]^-$.

3.3. Characterization of the triterpenoid saponins in the extract from A. julibrissin

The positive and negative modes TIC (total ion current) chromatograms of the sample are shown in Fig. 7. All major peaks corresponded to $[M+NH_4]^+$ and $[M+Na]^+$ ions in positive mode and $[M-H]^-$ and $[M-2H]^{2-}$ ions in negative mode. Twenty-eight compounds were identified by the features of their MS and MS/MS fragmentation patterns. Peaks 12, 11, 3, 1, 6, 5, 4, and 2 were identified as prosapogenin-9, prosapogenin-12, julibroside J_{25}, julibroside J_{20}, prosapogenin-3, prosapogenin-4, prosapogenin-10 and julibroside J_{22}, respectively, by comparing their MS features and retention times with those of the reference compounds.

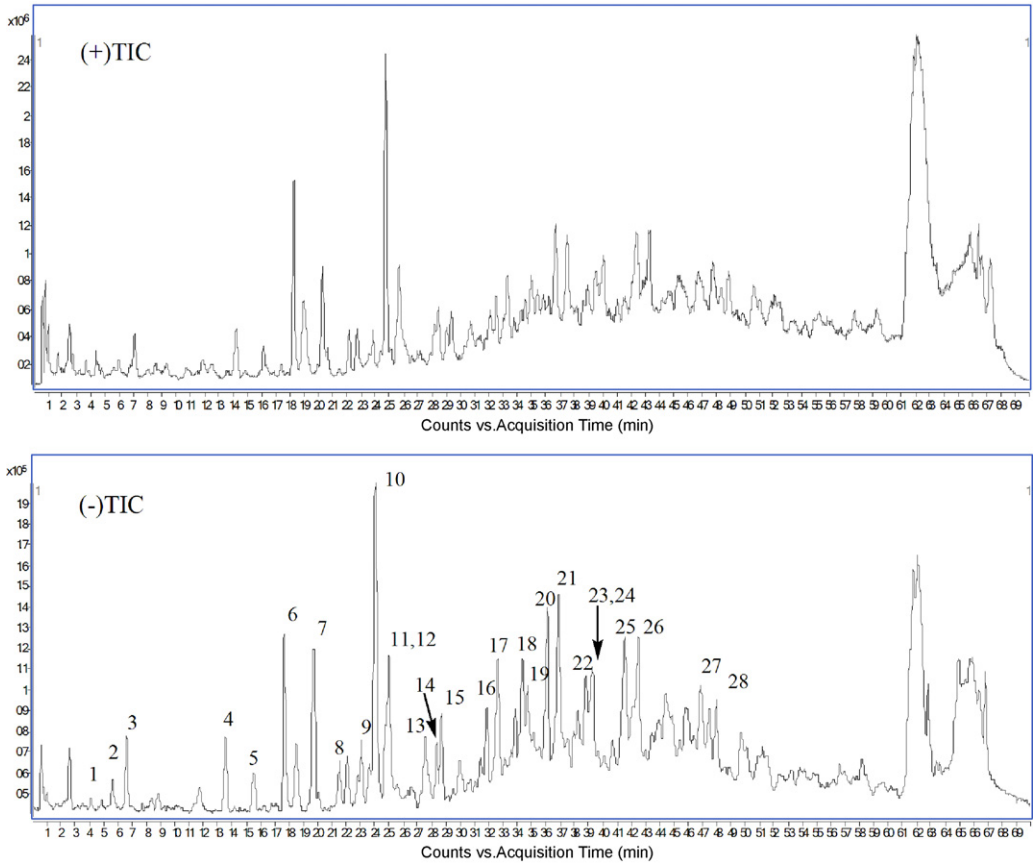

Fig. 7. Total ion current (TIC) chromatogram of the extract from *A. julibrissin* in positive and negative modes.

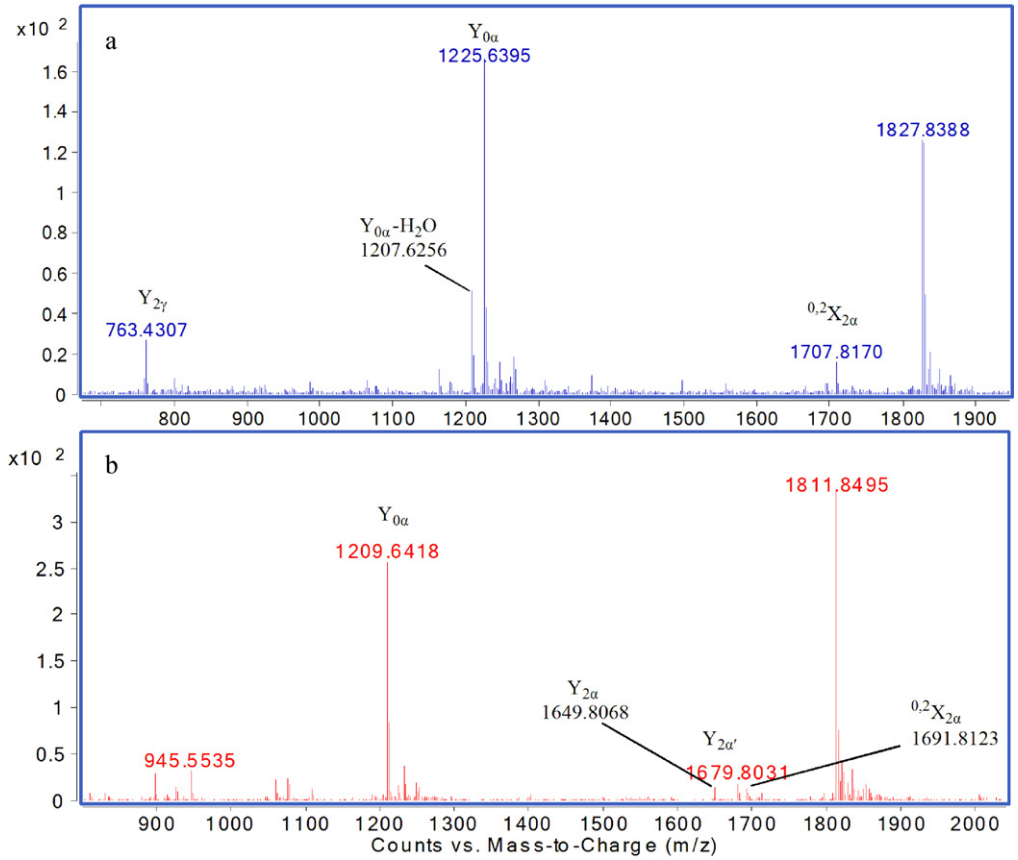

Fig. 8. (−) ESI-MS/MS spectrum of $[M-H]^-$ ion: (a) peak 9; (b) peak 13.

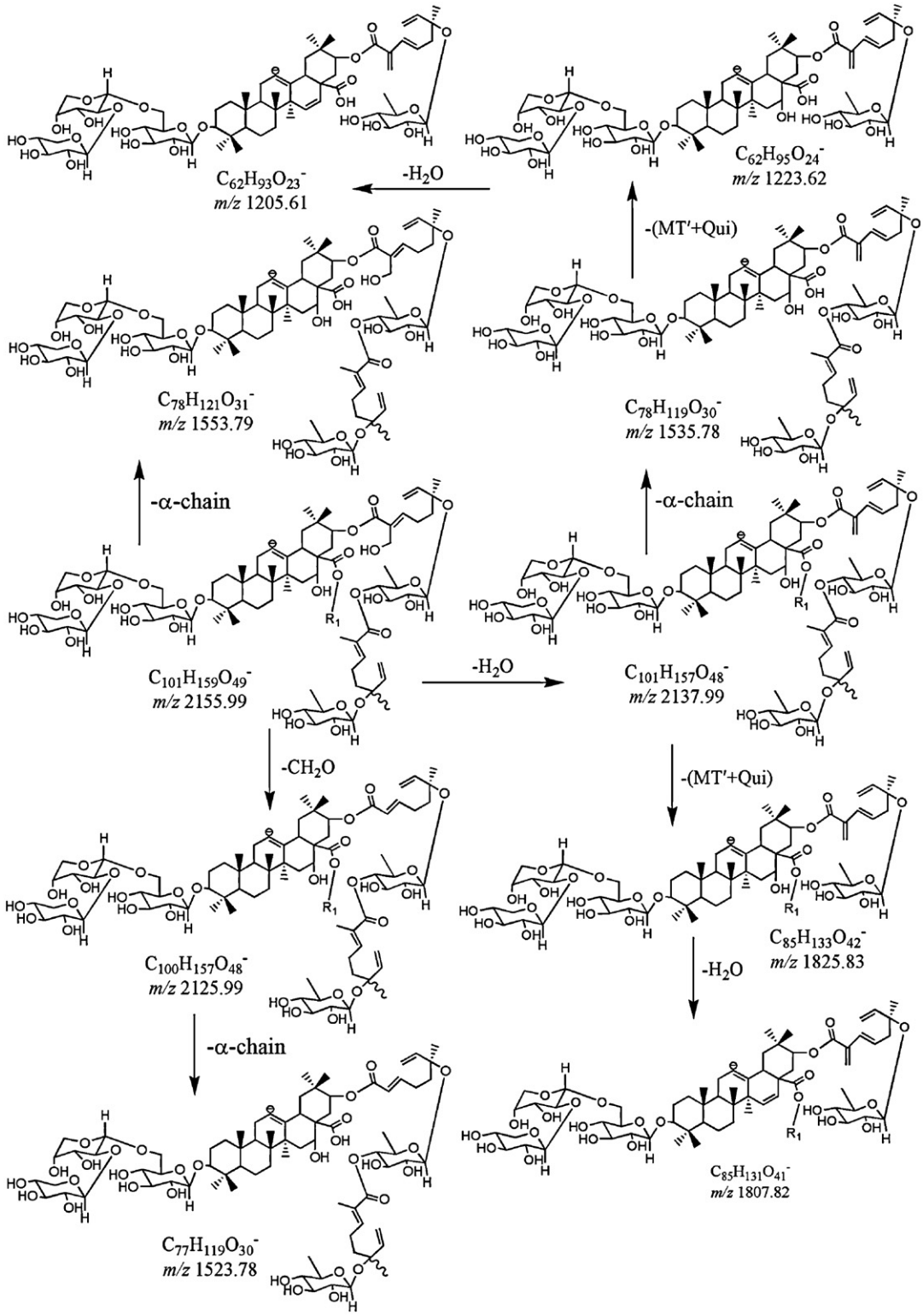

Fig. 9. Fragmentation pattern of peak 16.

3.3.1. Characterization of peak 7, 9, 13, 16, 17 and 23

Peak 7 produced $[M-H]^-$, $[M-2H]^{2-}$ ions at *m*/*z* 1827.8425 and *m*/*z* 913.4176 which corresponded to the molecular formula of $C_{85}H_{136}O_{42}$. In addition, $[M+NH_4]^+$ ions at *m*/*z* 1846.8823 was detected, but there were no $[M-2H-H_2O]^{2-}$ and $[M-2H-CH_2O]^{2-}$ ions in (−) ESI-MS. In the MS/MS spectrum, the $Y_{0\alpha}-H_2O$ (*m*/*z* 1207.6256), $Y_{0\alpha}$ (*m*/*z* 1225.6395) and $^{0,2}X_{2\alpha}$ (*m*/*z* 1707.8170) ions were observed (Fig. 8a). Deduced from these fragmentation features, the MT residue must not contain C_9–OH. Which according to the literature [5], has the same molecular weight as julibroside J_{26}. However, peak 7 contains a C_9–OH on MT residue, which is an isomer of julibroside J_{26}, and the hydroxyl group most probably located at the C-16 position. Therefore, the structure of peak 7 can be supposed as 3-*O*-[*β*-D-xylopyranosyl-(1 → 2)-*α*-L-arabinopyranosyl-(1 → 6)-*β*-D-glucopyranosyl]-21-*O*-[(6*S*)-2-*trans*-2,6-dimethyl-6-*O*-(*β*-D-quinovopyranosyl)-2,7-octadieno-

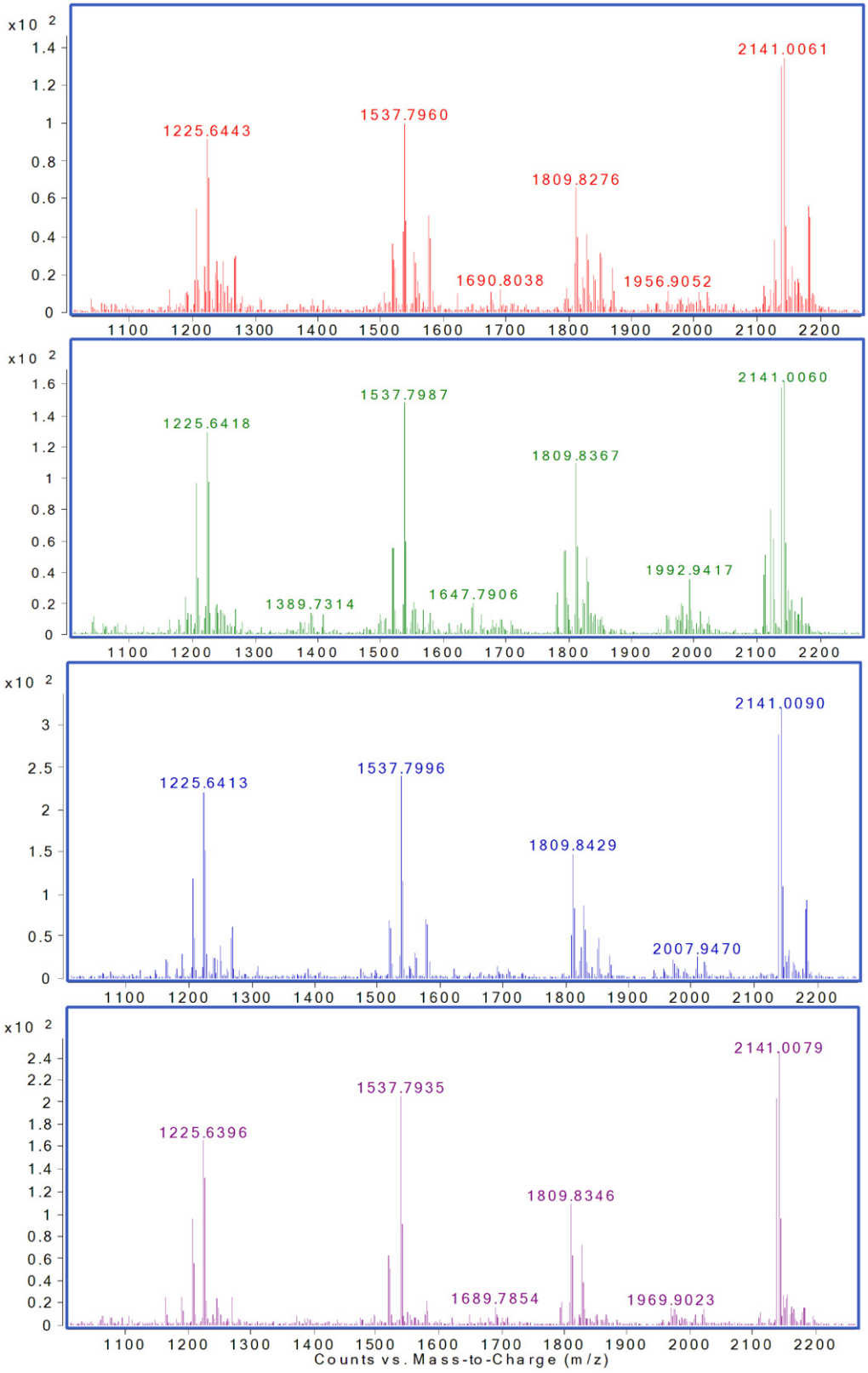

Fig. 10. (–) ESI-MS/MS spectrum of peak 18, 19, 25 and 26.

yl]-acacic acid -28-*O*-*β*-D-glucopyranosyl-(1 → 3)-[*α*-L-arabinofuranosyl-(1 → 4)]-*α*-L-rhamnopyranosyl-(1 → 2)-*β*-D-glucopyranosyl ester, which is a new compound.

Peak 9 gave $[M-H]^-$, $[M-2H]^{2-}$ and $[M+NH_4]^+$ ions at *m*/*z* 1811.8465, *m*/*z* 905.4190 and *m*/*z* 1830.8884 which corresponds to the molecular formula of $C_{85}H_{136}O_{41}$, which were all 16 Da less than that of peak 7. The MS/MS spectrum show $Y_{0\alpha}$ (*m*/*z* 1209.6418), $^{0,2}X_{2\alpha}$ (*m*/*z* 1691.8123), $Y_{2\alpha}$ (*m*/*z* 1649.8068) and $Y_{2\alpha'}$ (*m*/*z* 1679.8031). However, due to the fact that there is no $Y_{0\alpha}$–H_2O ion (see Fig. 8b), we can deduce that peak 9 does not

contain C_{16}–OH in the aglycone. Thus, the structure corresponds to 3-*O*-[*β*-D-xylopyranosyl-(1 → 2)-*α*-L-arabinopyranosyl-(1 → 6)-*β*-D-glucopyranosyl]-21-*O*-[(6*S*)-2-*trans*-2,6-dimethyl-6-*O*-(*β*-D-quinovopyranosyl)-2,7-octadienoyl]-16-deoxy-acacic acid-28-*O*-*β*-D-glucopyranosyl-(1 → 3)-[*α*-L-arabinofuranosyl-(1 → 4)]-*α*-L-rhamnopyranosyl-(1 → 2)-*β*-D-glucopyranosyl ester. It is also a new compound.

As shown in Table 1, peak 13 gave strong $[M-H]^-$ (*m*/*z* 1825.8627) and $[M-2H]^{2-}$ (*m*/*z* 912.4277) ions in the negative mode and a strong $[M+NH_4]^+$ (*m*/*z* 1844.9039) ion in the positive mode. Through the MS/MS fragment fragmentation pattern (Table 2) and the literature [3], peak 13 could be tentatively identified as prosapogenin-11, $C_{86}H_{138}O_{41}$.

Peak 16 and 17 produced $[M-H]^-$ (*m*/*z* 2155.99), $[M-2H]^{2-}$ (*m*/*z* 1077.49) and $[M+NH_4]^+$ (*m*/*z* 2175.04) ions, which implied that these two compounds have the same molecular formula, $C_{101}H_{160}O_{49}$. The MS/MS fragment ions are similar (see Table 2 and Fig. 9). According to the literature [9], julibroside J_1 and J_9 share the same molecular weight, they are diastereoisomers. According to the retention times reported in the literature, peak 16 was tentatively identified as julibroside J_1 and peak 17 was julibroside J_9.

The $[M-H]^-$ (*m*/*z* 2125.9856), $[M-2H]^{2-}$ (*m*/*z* 1062.4879) and $[M+NH_4]^+$ (*m*/*z* 2175.04) ions of peak 23 indicated that this compound had a molecular formula of $C_{100}H_{158}O_{48}$. In the MS/MS spectrum, $Y_{3\beta}$ (*m*/*z* 1827.8550), $Y_{0\alpha}$ (*m*/*z* 1523.7807), $Y_{3\beta}$–α-chain (*m*/*z* 1225.6643) and $Y_{3\beta}$–H_2O–α-chain (*m*/*z* 1207.6324) ions were observed. Thus, peak 23 was tentatively described as julibroside J_{35}.

3.3.2. Characterization of peak 14, 15, 18–22 and 24–28

All the (−) MS scan of peak 14, 15, 20 and 21 featured the $[M-H]^-$ at *m*/*z* 2170.01, corresponding to $C_{102}H_{162}O_{49}$, 14 Da higher than that of peak 16 (julibroside J_1) (see Table 1). The negative ESI-MS/MS spectrum gave the same fragment ions, such as $Y_{1\beta}$ (*m*/*z* 2152.00), $Y_{0\beta}$ (*m*/*z* 2140.00), $Y_{3\beta}$–H_2O (*m*/*z* 1839.84), $Y_{3\beta}$–H_2O (*m*/*z* 1821.84), $Y_{0\alpha}$ (*m*/*z* 1567.81), $Y_{0\alpha}$–H_2O (*m*/*z* 1549.79), $Y_{0\alpha}$–CH_2O (*m*/*z* 1537.79) and $Y_{3\beta}$–H_2O–α-chain (*m*/*z* 1237.64). According to the literature [14] and the cleavage rules, peak 20 and 21 were tentatively identified as julibroside J_5 and J_8. Peak 14 and 15 corresponds to the respective isomers of 20 and 21.

Peak 18, 19, 25 and 26 showed the same $[M-H]^-$, $[M-2H]^{2-}$ and $[M+NH_4]^+$ ions at *m*/*z* 2140.00, 1069.50 and 2159.04 respectively, which corresponded to the molecular formula of $C_{101}H_{160}O_{48}$, 16 Da less than that of peak 16 (julibroside J_1). In the MS/MS spectrum, the fragment ions at *m*/*z* 1827.84, 1809.83, 1537.80, 1519.80, 1225.64 and 1207.63 were due to the generation of $Y_{3\beta}$, $Y_{3\beta}$–H_2O, $Y_{0\alpha}$, $Y_{0\alpha}$–H_2O, $Y_{3\beta}$–α-chain and $Y_{3\beta}$–H_2O–α-chain ions (Fig. 10). From the MS/MS spectrum, the 16 Da less corresponds to a deoxidated of MT residue, which corresponds to julibroside J_{14} and J_{15} [6] and their respective isomers.

As summarized in Table 1, peak 22, 24, 27 and 28 also share the same $[M-H]^-$ at *m*/*z* 2154.01 in accordance with $C_{102}H_{162}O_{48}$, 14 Da higher than that of peak 18. In addition, the same $[M+NH_4]^+$ ions at 2173.06 was observed in the positive MS scan mode. However, peaks 22 and 27 produced two additional ions [$Y_{1\beta}$ (*m*/*z* 2135.99), $Y_{0\beta}$ (*m*/*z* 2124.01)] compared to peaks 24 and 28 in addition to $Y_{3\beta}$ (*m*/*z* 1841.87), $Y_{3\beta}$–H_2O (*m*/*z* 1823.85), $Y_{0\alpha}$ (*m*/*z* 1551.81), $Y_{0\alpha}$–H_2O (*m*/*z* 1533.81), $Y_{3\beta}$–α-chain (*m*/*z* 1239.65) and $Y_{3\beta}$–H_2O–α-chain (*m*/*z* 1211.64). According to the literature [2], peak 24 was tentatively identified as julibroside J_{16} and peak 28 was julibroside J_4. As for peaks 22 and 27, with a C_9–OH on MT residue, they were assumed to be hydroxyl positional isomers of julibroside J_{16} and J_4 respectively.

3.3.3. Characterization of peak 8 and 10

The $[M-H]^-$ ions of 8 (*m*/*z* 950.5120) and 10 (*m*/*z* 909.4853) were all less than 1000 Da and from the analysis of peaks 5 and 6, we can deduce that these two compounds have only one sugars chain each.

Peak 10 yielded the $[M-H]^-$ ion at *m*/*z* 909.4853 and $[M+NH_4]^+$ ion at *m*/*z* 928.5261, which all corresponded to the molecular formula of $C_{47}H_{74}O_{17}$. In the MS/MS spectrum, the fragment ions at *m*/*z* 777.4449 and 631.3895 were due to consecutive loss of one Xyl and one Fuc. Thus, peak 10 was tentatively identified as julibroside J_{A2} [20].

The $[M-H]^-$ and $[M+Na]^+$ ions at *m*/*z* 950.5120 and 974.5082 for peak 8 indicated that this compound had a molecular formula of $C_{49}H_{77}NO_{17}$. The observation of $[M-H-Ara]^-$ at *m*/*z* 818.4668 and $[M-H-Xyl-Fuc]^-$ at *m*/*z* 672.4178 in the MS/MS spectrum indicated that peak 8 was julibroside J_{A3} [20].

4. Conclusions

In the present study, fragmentation behavior of some triterpenoid saponins from *A. julibrissin* was summarized using negative ion UHPLC/ESI-Q-TOF-MS/MS spectra. On the basis of the analysis of the spectra fragmentation rules were proposed (see Section 3.2). Using these rules, twenty-eight compounds were identified, including eight new saponins. This UHPLC/ESI-Q-TOF-MS/MS method provided a rapid and accurate method for identification of triterpenoid saponins in crude extract from the stem bark of *Albizia julibrissin* Durazz. The present method will also be helpful for the rapid identification of similar triterpenoid saponins.

Acknowledgements

This work was supported by Program for Changjiang Scholars and Innovative Research Team in University (PCSIRT), Important Drug Development Fund, Ministry of Science and Technology of China (No. 2009ZX09311-002), Major Program of National Natural Science Foundation of China (No. 30830121) and Beijing Natural Science Foundation (No. 7093126).

References

[1] Pharmacopoeia Commission of People's Republic of China, Pharmacopoeia of People's Republic of China, vol. 1, People Health Press, Beijing, 2005, p. 97.
[2] D.H. Wei, S.Y. Qiao, Y.M. Zhao, Advances in study on bark of *Albizzia julibrissin*, China J. Chin. Mater. Med. 29 (2004) 619–624.
[3] T. Ikeda, S. Fujiwara, K. Araki, J. Kinjo, T. Nohara, T. Miyoski, Cytotoxic glycosides from *Albizia julibrissin*, J. Nat. Prod. 60 (1997) 102–107.
[4] K. Zou, Y.Y. Zhao, G.Z. Tu, J.H. Zheng, R.Y. Zhang, A new isomer of Julibroside J(2) from *Albizia julibrissin*, J. Asian Nat. Prod. Res. 1 (1998) 59–66.
[5] K. Zou, Y.Y. Zhao, G.Z. Tu, D.A. Guo, R.Y. Zhang, J.H. Zheng, A triterpenoid saponin from *Albizia julibrissin*, J. Asian Nat. Prod. Res. 1 (1999) 313–318.
[6] K. Zou, Y.Y. Zhao, B. Wang, D.Y. Li, S.Q. Cai, R.Y. Zhang, Structural identification of two diastereoisomeric saponins from *Albizia julibrissin*, Chem. J. Chin. Univ. 20 (1999) 1877–1882.
[7] K. Zou, Y.Y. Zhao, B. Wang, F. Xu, R.Y. Zhang, J.H. Zheng, Structural elucidation of julibroside j_{20}, Acta Pharm. Sin. 34 (1999) 522–525.
[8] K. Zou, J.R. Cui, Y.Y. Zhao, R.Y. Zhang, J.H. Zheng, A cytotoxic saponin with two monoterpenoids from *Albizia julibrissin*, Chin. Chem. Lett. 11 (2000) 39–42.
[9] K. Zou, Y.Y. Zhao, G.Z. Tu, J.R. Cui, Z.H. Jia, R.Y. Zhang, Two diastereomeric saponins with cytotoxic activityfrom *Albizia julibrissin*, Carbohydr. Res. 324 (2000) 182–188.
[10] K. Zou, B. Wang, Y.Y. Zhao, R.Y. Zhang, Isolation and identification of diastereoisomeric saponins with nine sugar moieties from *Albizia julibrissin*, Acta Chim. Sin. 62 (2004) 625–629.
[11] H. Liang, W.Y. Tong, Y.Y. Zhao, J.R. Cui, G.Z. Tu, An antitumor compound julibroside J(28) from *Albizia julibrissin*, Bioorg. Med. Chem. Lett. 15 (2005) 4493–4495.
[12] K. Zou, J.R. Cui, F.X. Ran, B. Wang, Y.Y. Zhao, R.Y. Zhang, J.H. Zheng, Structures and activity of two novel saponins from *Albiza julibrissin*, Chin. J. Org. Chem. 25 (2005) 654–659.
[13] K. Zou, J.R. Cui, B. Wang, Y.Y. Zhao, R.Y. Zhang, A pair of isomeric saponins with cytotoxicity from *Albizzia julibrissin*, J. Asian Nat. Prod. Res. 7 (2005) 783–789.
[14] K. Zou, W.Y. Tong, H. Liang, J.R. Cui, G.Z. Tu, Y.Y. Zhao, R.Y. Zhang, Diastereoisomeric saponins from *Albizia julibrissin*, Carbohydr. Res. 340 (2005) 1329–1334.

[15] L. Zheng, J. Zheng, L.J. Wu, Y.Y. Zhao, Julibroside J(8)-induced HeLa cell apoptosis through caspase pathway, J. Asian Nat. Prod. Res. 8 (2006) 457–465.
[16] L. Zheng, J. Zheng, Y.Y. Zhao, B. Wang, L.J. Wu, H. Liang, Three anti-tumor saponins from *Albizia julibrissin*, Bioorg. Med. Chem. Lett. 16 (2006) 2765–2768.
[17] K. Zou, Y.Y. Zhao, R.Y. Zhang, A cytotoxic saponin from *Albizia julibrissin*, Chem. Pharm. Bull. 54 (2006) 1211–1212.
[18] T.H. Xu, H.T. Li, Y.J. Xu, H.F. Zhao, S.X. Xie, D. Han, Y.S. Si, Y. Li, J.Z. Niu, D.M. Xu, A new triterpenoid saponin from *Albizia julibrissin* Durazz, J. Asian Nat. Prod. Res. 10 (2008) 771–775.
[19] L. Zheng, J. Zheng, Q.Y. Zhang, B. Wang, Y.Y. Zhao, L.J. Wu, Three new oleanane triterpenoid saponins acetylated with monoterpenoid acid from *Albizia julibrissin*, Fitoterapia 81 (2010) 859–863.
[20] J. Kinjo, K. Araki, K. Fukui, H. Higuchi, T. Ikeda, T. Nohara, Y. Ida, N. Takemoto, M. Miyakoshi, J. Shoji, Six new triterpenoidal glycosides including two new sapogenols from Albizziae cortex. V, Chem. Pharm. Bull. 40 (1992) 3269–3273.
[21] L.B. Ma, G.Z. Tu, S.P. Chen, R.Y. Zhang, L.H. Lai, X.J. Xu, Y.Q. Tang, NMR determination of the structure of Julibroside J_1, Carbohydr. Res. 281 (1996) 35–46.
[22] J. Kinjo, K. Fukui, H. Higuchi, T. Nohara, The first isolation of lignin tri- and tetra-glycosides, Chem. Pharm. Bull. 39 (1991) 1623–1625.
[23] J. Kinjo, H. Higuchi, K. Fukui, T. Nohara, Lignoids from Albizziae cortex. II, Chem. Pharm. Bull. 39 (1991) 2952–2955.
[24] H. Higuchi, K. Fukui, J. Kinjo, T. Nohara, Four new glycosides from Albizziae cortex. III, Chem. Pharm. Bull. 40 (1992) 534–535.
[25] M. Kaneta, H. Hikichi, S. Endo, Identification of flavones in sixteen leguminosae species, Agric. Biol. Chem. 44 (1980) 1407.
[26] H. Higuchi, J. Kinjo, T. Nohara, An arrhythmic-inducing glycoside from *Albizzia julibrissin* Durazz. IV, Chem. Pharm. Bull. 40 (1992) 829–831.
[27] G. Montoya, G.J. Arango, M. Unger, U. Holzgrabe, *O*-Glycoside sequence of pentacyclic triterpene saponins from *Phytolacca bogotensis* using HPLC-ESI/multi-stage tandem mass spectrometry, Phytochem. Anal. 20 (2009) 465–467.
[28] J.B. Zhu, X.J. Guo, S.P. Fu, X.L. Zhang, X.M. Liang, Characterization of steroidal saponins in crude extracts from *Dioscorea zingiberensis* C.H. Wright by ultra-performance liquid chromatography/electrospray ionization quadrupole time-of-flight tandem mass spectrometry, J. Pharm. Biomed. Anal. 53 (2010) 462–474.
[29] L. Novakova, L. Matysova, P. Solich, Advantages of application of UPLC in pharmaceutical analysis, Talanta 68 (2006) 908–918.
[30] L.F. Han, B.P. Ma, H.S. Zh, X.B. Song, X.M. Gao, L.P. Kang, C.Q. Xiong, Y. Zhao, D.W. Tan, ^{1}H and ^{13}C NMR assignments for four triterpenoid saponins from Albizziae cortex, Magn. Reson. Chem. 46 (2008) 1059–1065.
[31] L. Wang, Y. Sun, F. Du, W. Niu, T. Lu, J. Kan, F. Xu, K. Yuan, T. Qin, C. Liu, C. Li, 'LC-electrolyte effects' improve the bioanalytical performance of liquid chromatography/tandem mass spectrometric assays in supporting pharmacokinetic study for drug discovery, Rapid Commun. Mass Spectrom. 21 (2007) 2573–2584.
[32] X. Qiao, X. Zhang, M. Ye, Y.F. Su, J. Dong, J. Han, J. Yin, D.A. Guo, Rapid characterization of triterpene saponins from *Conyza blinii* by liquid chromatography coupled with mass spectrometry, Rapid Commun. Mass Spectrom. 24 (2010) 3340–3350.